The depth-varying response of coastal circulation and water levels to 2D radiation stress when applied in a coupled wave-tide-surge modelling system during an extreme storm.

Submission for Coastal Engineering

Jennifer M. Brown [a,*], Rodolfo Bolaños [a,b], Judith Wolf [a]

[a] National Oceanography Centre, Joseph Proudman Building, 6 Brownlow Street, Liverpool, L3 5DA, UK.

[b] Now at DHI, Agern Alle 5, Hørsholm 2970, Denmark.

[*] Corresponding author *Phone*: +44 (0) 151 795 4971, *Fax*: +44 (0) 151 795 4801, *Email*: jebro@pol.ac.uk (J.M. Brown)

Abstract

During storm events wave setup in shallow regions can contribute significantly to the total water elevation, radiation stress can also generate alongshore drift influencing sediment transport. In low lying coastal regions this generates the potential for flood inundation and morphological change. A coupled tide-surge-wave modelling system is therefore required for accurate forecasting. Liverpool Bay, UK, is taken as a case study because it has a resource of observations and incorporates three estuaries, thus providing conditions to assess the model performance both at the open coast and within estuarine environments. The model covers a region encompassing depths from about 50 m below the mean tidal level to shallow wetting and drying regions, and has previously given good wave and surge hindcasts both for individual storm events and multi-year studies.

The present study builds on an already accepted model, to include and assess the spatial influence of 2D radiation stress when implemented in a 3D circulation model. The results show that the method is computationally efficient, so relevant for operational use, and also provides a plausible solution. The varied influence of radiation stress across a coastal domain is demonstrated, with larger impact at an estuary mouth and along the open coast, while having lesser impact within an estuary and further offshore.

Keywords: Tide-surge-wave modelling, Shallow water, Wind waves, POLCOMS-WAM, Radiation stress, Wave setup, Liverpool Bay.

1. Introduction

To conserve momentum in shallow water, a force balancing any change in momentum is generated. The excess momentum flux due to surface waves is defined as radiation stress (Longuet-Higgins and Stewart, 1964). In shallow regions, the presence of waves can increase or decrease the mean water level, which is known as wave setup or wave set-down. This change in water level is an integrated effect over a region caused by gradients in radiation stress. Often waves do not approach a coastline perpendicularly and a wave-induced alongshore current is also manifested (Longuet Higgins, 1970a and b). During storm conditions, increased water levels arise due to the combined influence of direct meteorological forcing and wave setup, which together generate a storm surge. It has been known for considerable time (Harris, 1963) that at the open coast wave setup can contribute to storm surge levels, during extreme storm events (e.g. with 100 year return period) the wave setup can contribute 30-60% of the total storm surge elevation (Dean and Bender, 2006). In addition, the morphological evolution of sandy beaches can depend on sediment transport driven by the alongshore current (Sherman, 1988). Radiation stress has played an important role in the studies of nearshore currents, wave setup, wave set-down and rip currents, commonly using 2D (depth-averaged) radiation stress in modelling approaches (Mastenbroek et al., 1993; Sheng et al., 2010). In this approach the radiation stress, S_{ij}, is expressed as:

$$S_{ij} = \rho g \int_{o}^{2\pi} \int_{0}^{\infty} \left\{ \frac{c_g}{c} \frac{k_i k_j}{k^2} + \left(\frac{c_g}{c} - \frac{1}{2} \right) \delta_{ij} \right\} \times F(f,\theta) df d\theta \tag{1}$$

Where ρ = water density, g = acceleration due to gravity, c_g = wave group velocity, c = the wave phase speed, k = the wave number, δ = the Kronecker delta function, F = the wave spectrum, f = the wave frequency, θ = the wave direction and i,j = the direction components.

Including 2D radiation stress within models has improved water level modelling (Roland et al., 2009), modified inundation simulations (Xie et al., 2008) and enabled the study of wave-induced currents and wave setup (Pleskachevsky et al., 2009). However, 3D effects can also be important, since radiation stress is induced by surface waves and is thus not distributed equally in the vertical; recently more attention has been paid to this, e.g., Ardhuin et al. (2008a, 2008b), Bennis et al. (2011), Bennis and Ardhuin (2011), Mellor (2003, 2005, 2008, 2011a, 2011b, 2011c, 2013) and Xia et al. (2004). Recent modelling studies (Brown, 2010; Brown et al., 2011; Bolaños et al., 2011a) have found that the inclusion of a 3D radiation stress method (see Mellor, 2003; 2005) increased the hindcast water level and modified the current field during both extreme and more typical conditions. However, the reliability of the method used (Mellor's approach) has been questioned (Brown et al., 2011), in particular the robustness of the influence of radiation stress on the vertical current profile (Bennis et al., 2011) and the accuracy of the vertical pressure term (Ardhuin et al., 2008a, 2008b). New 3D radiation stress methods are presently being developed (Mellor, 2008; 2011; Bennis et al., 2011) in addition to the application of vortex force formulation (Kumar et al., 2012; Moghimi et al., in press). Earlier work (Mastenbroek et al., 1993) has shown that radiation stress in 2D can give a good surge-setup hindcast. While 3D methods are undergoing rigorous validation (e.g., Kumar et al., 2011; Moghimi et al., in press; Sheng and Li, 2011) this study assesses the contribution of the 2D method across a coastal region, using model-observation comparisons as validation where available. At present, 3D radiation stress methods have limited application and are not robust over a full regional application with unrealistic flow generation in certain areas (Kumar et al., 2011). Stable 2D radiation stress methods are therefore still used within depth-integrated (2D) circulation models to simulate extreme wave-circulation conditions (e.g. Dietrich et al., 2012). Here, the aim is to identify if 2D methods are adequate, when implemented in a 3D circulation model, while there is still debate on the accuracy and suitability of 3D methods and also to identify where radiation stress has most influence across a region of: estuaries, open coast and the nearshore zone.

To assess the importance of 2D radiation stress in 3D hydrodynamic models, this study looks at wave setup and wave-induced currents during an extreme storm event across a shoaling region of wave-influence in the UK, Liverpool Bay (Fig. 1). This area covers a region of gradually decreasing depths from about 50 m below the mean tidal level offshore, to the coast. Within the bay there are three estuaries along with large areas of intertidal beaches and banks. This allows a range of shallow water environments to be studied. An extreme storm event (~2 m surge elevation and ~5.2 m H_{m0} wave height), occurring on the 18th January 2007 is hindcast using the

Proudman Oceanographic Laboratory Ocean Modelling System coupled to the WAve Model (POLCOMS-WAM). This system has proven to give a good model hindcast for the Irish Sea (Brown et al., 2010) and within Liverpool Bay (Bolaños et al., 2011a), especially for this event (Brown, 2010; Brown et al., 2011). This model therefore provides a good basis for further development. The event considered is one of the largest storms, with a complete set of coincidental wave, water level and current observations, to have occurred in the past decade for this study site. This event is associated with the easterly passage of a depression across the north of Ireland and over Scotland (Brown and Wolf, 2009). The observed atmospheric pressure at Hilbre Island ranged from 974 to 999 mb during the event. The storm track produced veering winds from southwest to west, which were observed to peak at 17.3 m/s at the Hilbre Island met station (Brown, 2010). In response to the meteorological forcing the surge exceeded levels of 2 m along the northwest English coast, while the significant wave height (H_{m0}) offshore reached 4.95 m during this 25 hour storm period. The nearshore currents during this study period were of the order of 1 m/s at two mooring sites (A and B, Fig. 1) and predominantly in an east-west direction. At this time the astronomical tidal range was 6.66 m, which is just above the mean tidal range (6.25 m). To fully assess the model skill, and the importance of the radiation stress, observed data have been obtained from the Coastal Observatory (COBS, Howarth et al., 2006; http://cobs.noc.ac.uk). The following observations are available at specified locations given in Fig. 1: total surge elevations at two coastal tide gauges (Hilbre and Liverpool), wave heights and periods at two wave buoys (WaveNet and Triaxys) and vertical current profiles at two fixed mooring sites (A and B).

This study aims to extend the previous research of Brown (2010), Bolaños et al. (2009; 2011a; 2011b) and Brown et al. (2011) by investigating the regional influence of radiation stress during extreme storm events in shallow, wave-influenced regions. A 2D method is assessed to determine the contribution of wave setup to storm surge simulations and assess its suitability for operational use. The POLCOMS-WAM model has been modified (Section 2) to include 2D radiation stress. The model results are validated and compared with previous 3D simulations in Section 3. The results are used to determine coastal locations where radiation stress may be important under storm conditions. A discussion of the different 2D modelling approach is presented, comparing the numerical stability of these methods over the full domain of a complex coastal region. Their application in operational models is considered in Section 4, before concluding, in Section 5, that the 2D method is appropriate for accurate, efficient computation.

2. Modelling Methods

2.1. The modelling system

To simulate wave-tide-surge conditions a nested modelling approach is used to propagate surge and waves across the continental shelf and within the Irish Sea to the study area. Three structured model grids are used: the operational Continental Shelf model (~12 km resolution), the Irish Sea model (~1.8 km resolution) and the Liverpool Bay model (~180 m resolution, Fig. 1). The Irish Sea and Liverpool Bay models were set up for the study of this storm event, while the Continental Shelf model (Flather, 1994) is run daily at the UK Met Office to provide operational tide-surge forecasts. Here, the hindcast tide-surge data from this model is utilized as hourly time series boundary conditions for the Irish Sea model. In turn, the Liverpool Bay model boundary is forced with tide-surge conditions every 30 minutes and 2D spectral wave conditions every hour from the coupled Irish Sea model. Each model is driven by the same meteorological forcing, which consists of hourly wind and pressure data with ~12 km resolution from the (mesoscale) UK Met Office Unified Model (MetUM) North Atlantic European (NAE) model. The modelled conditions for this event are output hourly for waves, surface elevation and 3D circulation.

Since density stratification is generally considered unimportant in mid-latitude winter storm surge and wave modelling, freshwater influence has been ignored and the temperature (10 °C) and salinity (35 PSU) fields, and therefore density, are kept constant. The 3D circulation model POLCOMS (detailed in Holt and James, 2001), is formulated on an Arakawa B-grid, solving scalar quantities at grid vertices and vector quantities centrally within the grid cells. To enable wave effects to be included, POLCOMS is coupled to a wave model at the medium and high resolution model grids. To this end, the third generation spectral wave model (WAM) is used. WAM, originally developed for deep water application (see Komen et al., 1994), has been further developed to enable nearshore wave simulation (Monbaliu et al., 2000). The coupling was applied such that a 2-way exchange of information occurred every 200 s for the Irish Sea model and every 30 s for the Liverpool Bay model. The interactions considered for tide-surge-wave simulation were as follows. Time varying current and depth information was passed to WAM, while surface and bottom roughness were passed back to POLCOMS (Osuna and Wolf, 2005) along with the radiation stress (Bolaños et al., 2009; 2011b). In WAM the coupling procedure introduces time varying depth and 3D current fields (Bolaños et al., 2009; 2011b; Mellor, 2003; 2005; Kirby and Chen, 1989), which influence refraction and allow inclusion of a wave-current bottom friction, Doppler shift of the wave field and an ‘effective wind’ due to the moving frame of reference (surface current). In POLCOMS the radiation stress is added to the equations of motion to allow for wave-induced currents and wave setup (see below Eq. 2 and 3), while the surface and bottom roughness is enhanced due to the presence of waves modifying the bottom friction and wind stress. Extensive testing and validation of the coupling procedures has recently been performed by Brown et al. (2011). The model is again applied here to the Irish Sea to simulate wave generation by wind, while accounting for bottom friction, whitecapping, wave-wave interactions and refraction due to depth and current. Further to these terms, depth-induced wave breaking and radiation stress were included in the Liverpool Bay model. Wave parameters were computed on the same grid as POLCOMS at the same location as the scalar quantities. Velocity and wave-related stress terms were interpolated between grid vertices to central points within the models to enable correct coupling.

Initially a 3D radiation stress method (Mellor, 2003; 2005) was coded by Bolaños et al. (2009; 2011b), and has been set up for a shallow water application (Brown, 2010; Brown et al., 2011). New 3D developments are now available (Mellor, 2008; 2011a; 2011b; 2011). However, these latter methods can lead to spurious accelerations in intermediate water depths (Bennis et al., 2011), in particular outside the surf zone (Bennis and Ardhuin, 2011). The generation of unrealistic circulation (Kumar et al., 2011) leads to doubtful coastal application (Moghimi, in press) and has led to further developments (Mellor, 2013). We therefore investigate the validity of using the 2D radiation stress terms of Mastenbroek et al. (1993) as a robust alternative. Ozer et al. (2000) incorporated calculation of this 2D radiation stress term within WAM. We extend this work by coupling the depth-averaged stress terms back into POLCOMS uniformly over the water column, as described below. This is important for obtaining spatially realistic wave setup over a region.

POLCOMS solves the incompressible, hydrostatic, Boussinesq equation by separation into depth-varying (3D) and depth-integrated (2D) parts (see Holt and James, 2001, for the original model terms and description). The total velocity is then the sum of the depth-mean and depth-varying velocity components, over 32 and 10 vertical sigma levels within the water column of the Irish Sea and Liverpool Bay models respectively. Bolaños et al. (2009; 2011b) added the 3D radiation stress terms into the depth-varying momentum equation. These are now replaced with 2D radiation stress terms, which are added into the depth-mean momentum equation, in Cartesian coordinates the equations solved read as:

$$\frac{\partial u}{\partial t} + u\frac{\partial u}{\partial x} + v\frac{\partial u}{\partial y} - fv = -g\frac{\partial \eta}{\partial x} - \frac{1}{\rho}\frac{\partial P_a}{\partial x} + \frac{1}{\rho h}\left(\tau_s^x - \tau_b^x\right) + \frac{\partial}{\partial x}\left(A_h\frac{\partial u}{\partial x}\right) + \frac{\partial}{\partial y}\left(A_h\frac{\partial u}{\partial y}\right) - \frac{1}{\rho h}\left(\frac{\partial S_{xx}}{\partial x} - \frac{\partial S_{xy}}{\partial y}\right) \quad \ldots(2)$$

$$\frac{\partial v}{\partial t} + u\frac{\partial v}{\partial x} + v\frac{\partial v}{\partial y} + fu = -g\frac{\partial \eta}{\partial y} - \frac{1}{\rho}\frac{\partial P_a}{\partial y} + \frac{1}{\rho h}\left(\tau_s^y - \tau_b^y\right) + \frac{\partial}{\partial x}\left(A_h\frac{\partial v}{\partial x}\right) + \frac{\partial}{\partial y}\left(A_h\frac{\partial v}{\partial y}\right) - \frac{1}{\rho h}\left(\frac{\partial S_{yx}}{\partial x} - \frac{\partial S_{yy}}{\partial y}\right) \quad \ldots(3)$$

Which are solved alongside the continuity equation:

$$\frac{\partial (hu)}{\partial x} + u\frac{\partial (hv)}{\partial y} = -\frac{\partial \eta}{\partial t} \quad \ldots(4)$$

Where x,y = the orthogonal directional components, u,v = the depth-integrated current components, η = surface elevation, f = the Coriolis parameter, h = the total water depth, P_a = atmospheric pressure, τ_s = surface stress, τ_b = bottom stress, A_h = the horizontal diffusion coefficient and S_{ij} = the radiation stress tensor (with $i,j = x,y$). The radiation stress is updated with each call to the wave model (every 30 s), which is where the stresses themselves are calculated. By imposing the radiation stress within the momentum equations a change in the current field is imposed, which causes an adjustment in surface elevation for the system of equations (Eq. 2 – 4) to remain in balance. The coupled POLCOMS-WAM model is designed to run on a parallel computer system (Ashworth et al., 2004) for high resolution modelling such as this. To compare the efficiency of the radiation stress method in 2D against the previous (Brown et al., 2011) 3D method the model simulation has been run on the same computing facility. The Liverpool Bay hindcast used 256 computer processors from the UK's supercomputing service: HECToR (High-End Computing Terascale Resource, *http://www.hector.ac.uk/*), to enable a 1 day spin-up and a 1 day tide-surge-wave simulation in approximately 12 hours of real time.

2.2. Validation Methods

The model hindcasts were validated at hourly intervals over the 25-hour storm period. The surge elevation was validated at two coastal tide gauges (Hilbre and Liverpool, Fig. 1) and two offshore mooring sites (Site A and B, Fig. 1) where pressure sensors were available. The wave height and period were validated at an offshore and nearshore wave rider buoy (WaveNet and Triaxys, Fig.1). The currents were validated at the two offshore sites (Site A and B, Fig. 1) using Acoustic Doppler Current Profilers (ADCP), which measured the vertical current profile. For validation purposes the following metrics are applied to the hourly data for the full 25-hour storm period:

$$Mean\ Bias = \overline{Modelled} - \overline{Observed} \qquad \ldots(5)$$

$$Peak\ Bias = \widehat{Modelled} - \widehat{Observed} \qquad \ldots(6)$$

$$RMSE = [\overline{(Modelled - Observed)^2}\ ]^{1/2} \qquad \ldots(7)$$

where an over-bar denotes the mean values and a circumflex denotes the maximum value. The (*Mean or Peak*) *Bias* represents under- or over-prediction of the model quantity compared with the observation and the *RMSE* is the root-mean-square error of the model hindcast. For all variables assessed, the *RMSE* is used to determine the average accuracy over the full period. For waves and surge the maximum values are considered important for storm forecasting and coastal storm impact so the *Peak Bias* is also measured. For currents the *Mean Bias* was calculated because it is the net residual current that is important, for example, for sediment transport studies.

In this application the range in observed values over the 25 hour study period is used to specify if the model performance is excellent, good, acceptable or unacceptable, by applying the following thresholds to the metric values: <10%, 10-30%, 30-50% and >50%. During the 25-hour period considered the range observed in total surge values (shown in Fig. 2 and 3) is: 1.9 m at Hilbre, 2.1 m at Liverpool, 1.5 m at Site A and 1.2 m at Site B. The range (between maximum and minimum values) in the observed depth-averaged current (Fig. 7) at Site A and B is 1.7 m/s and 1.4 m/s for the u-component respectively and 0.4 m/s and 0.3 m/s for the v-component respectively. At the WaveNet location the observed H_{m0} and T_p (Fig. 8, left column) have ranges of: 4.2 m and 7.3 s. At the Triaxys location the observed H_{m0} and T_p (Fig. 8, right column) have the ranges: 2.3 m and 6.2 s.

3. Results

3.1. Surge and wave setup

The observed surge consists of the response to the direct meteorological forcing and wave-induced setup. The model hindcasts are validated (Table1) at two coastal tide gauges (O(10 m) deep), where the observed surge is available. The residuals are determined by removing the predicted tide for these locations using tidal constituents obtained from analysis of coastal tide gauge data. At these locations it is found that both the POLCOMS-WAM model with 2D radiation stress (PW – 2Dr), and without consideration of radiation stress (PW), perform well. The inclusion of 2D radiation stress improves the maximum value but has little effect at any other time during the storm. Previously the inclusion of 3D radiation stress (Brown et al., 2011) has shown quite different results. Although the maximum value (*Peak Bias*) was fairly good, it occurred too early and the influence of radiation stress occurred for a much longer proportion of the storm (10

– 15 hrs). Here, the inclusion of 2D radiation stress has negligible impact on the computation time, while the 3D radiation stress reduces computational efficiency, in this case by 25% (Table 1), which is equivalent to 1.5 hours per simulated day.

The POLCOMS-WAM simulation with 2D radiation stress (Fig. 2) implies that wave setup does not significantly contribute to the surge at the tide gauge locations or offshore, the model runs including 2D radiation stress being similar to that without. This is not unexpected as coastal tide gauges although influenced by surge are usually sheltered from waves and in deep water, in this case within estuaries where wave activity is limited, since the waves mostly break on the shoals at the mouth.

To validate the surge further offshore, pressure sensor data for a two month period at Sites A (~23 m depth) and B (~29 m depth) are analysed. T-tide, a classical tidal harmonic analysis package (Pawlowicz et al., 2002), is used to remove the tidal component from the observed water levels, to enable the residual to be determined. All the 45 available major tidal constituents, as well as shallow water constituents, are considered at these offshore locations, giving the surge (tidal residual) seen in Figure 3. Over a long period (at least a year) the mean tidal residual will be zero; however for short periods (e.g., the two month winter period observed or 1 day period modelled) the residual is not quite zero due to seasonal/daily storm effects. Since the observed mean will be closer to zero due to the longer period considered than that modelled, a shift in the surge level between observed and modelled data occurs (~0.4 m). To enable meaningful validation between model and observation, the mean residual from each model simulation, over the 25-hour storm period, has been applied to the observed data, such that the mean value is equal between modelled and observed surge for each simulation validated. At these locations it is clearly seen that the model accurately simulates the trend in the surge, although the model accuracy (Table 1) is reduced with distance from the coast. The results show that offshore the surge is smaller (about 50% reduction in the maximum value at the mooring Sites A and B compared with the tide gauges) and the negligible difference between runs with and without 2D radiation stress demonstrate that (as expected) wave setup is unimportant in offshore water depths >20 m.

Offshore (Fig. 3, Site A and B) the surge is over predicted during the storm and inshore (Fig. 2) it can be either over-predicted (Hilbre) or under-predicted (Liverpool). The over prediction is most likely to be the result of over-predicted wind speeds used to force the model during the storm (as shown by Brown, 2010). The mean value of wind-speed is over-predicted by 1.9 m/s at Hilbre. The coastal accuracy is also limited by the accuracy of the bathymetry, which is highly mobile in the estuary regions, used within the model. The common under-prediction of the surge is due to the model boundary conditions as this also occurs in the Irish Sea model (see Brown and Wolf, 2009). This error could be related to inaccuracy in the storm track, size or speed influencing the meteorological surge generation over the European Continental Shelf, or incorrect tuning of wind-stress.

The fully coupled model is used to obtain estimates of the contribution of wave setup across this varied domain, including estuary systems, open coast and the nearshore region of wave shoaling (Fig. 4). Since the model is coupled in 2-way the circulation model can properly respond in a dynamical way to the radiation stress. A computed setup that is too large can occur in the enclosed (estuary) regions in the absence of a circulation response to the change in elevation (2-way model coupling). It appears that with 2-way coupling wave setup has a more significant contribution in shallow open coastal areas than within an estuary. The maximum wave setup values are 0.15 m on the shallowest banks in the Ribble and 0.08 m nearshore. The patterns in maximum wave setup (Fig. 4b) seem to be related to the bathymetry (Fig. 1) rather than the wave field (Fig. 4a), as the channel into the Mersey can be clearly distinguished. Data collected by King et al. (1990) suggests wave setup at the coast, for 1 to 2.5 m waves in 10 m of water approaching a coast in SW England bordering the Irish Sea, is between 0.1 and 0.25m. These observations are comparable to the PW-2Dr hindcast. However, without observations, the model results are merely suggestive. This highlights the need for measurements of water level in shallow open coast locations, where radiation stress has greatest impact.

The maximum meteorological surge level across the domain is presented by Brown (2010). Here the ratio of the maximum wave setup to the maximum meteorological surge is shown (Fig. 4c). This demonstrates that the locations where the wave setup (relative to the meteorological surge levels) is most noticeable, are: (i) the open coast and (ii) at the mouth of an estuary, especially around the shoals. The maximum wave setup is at most ~ 5% of the maximum meteorological surge across the domain. For this event the meteorological surge therefore has greatest influence increasing the water levels during this storm. For the estuaries with open mouths (the Dee and Ribble) the wave setup is able to influence the estuarine water levels, whereas in the Mersey, with its narrow mouth, only the meteorological surge component influences the estuary system.

3.2. Currents

In this section both the total and wave-induced current fields are compared with observations. The currents induced by radiation stress are extracted from the total modelled current field (POLCOMS-WAM with radiation stress); by subtracting the current field in which the radiation stress is not considered (POLCOMS-WAM). Currents during the studied period at the two observation sites (A and B, with depths of ~23 and ~29 m, Fig. 1) are mainly controlled by the tides with maxima in agreement with flood and ebb flows (observation, Fig. 5). Weak variation in the vertical current profile is present during the second low tide when the peak of the storm surge occurred. This is more evident at the shallower location, Site A. The POLCOMS-WAM model (PW, Fig. 5) is able to reproduce the general patterns of the horizontal current, which are clearly dominated by the tides. The inclusion of 2D radiation stress has a vertically variable influence (see Fig. 6 for wave-induced currents), as the 3D circulation model responds to the modified depth-averaged flow. However, no significant changes are observed in the total current field (Fig. 5). The wave-induced currents (Fig. 6) are greater during the falling and rising tide as the storm passes and wave heights decay (15 – 22.5 hrs). Section 3.4 goes on to show how this is related to the tidal influence on the gradients in the nearshore wave field, which cause the radiation stress that generates these currents. The 2D radiation stress has more influence at Site A (Fig. 6), which is shallower than Site B and closer to the area of banks located at the mouth of the Mersey estuary.

Validation of the depth-averaged current at the offshore locations (Table 2, Fig. 7) shows good agreement between model and observation before radiation stress is considered. The inclusion of 2D radiation stress has little effect on the model accuracy. In both simulations the *Mean Bias* shows the models to consistently under-predict the observed current components at the offshore sites (A and B, Table 2). This could be related to a slight error in the tidal axis orientation, which would produce marked differences in the minor (north) velocity component. Since these error metrics look at the average accuracy over the 25 hour study period the instantaneous improvements at certain depths by considering radiation stress are not so evident, due to smoothing (over depth and time).

3.3. Waves

The wave conditions are validated in Table 3 at the estuarine (~12 m deep) and offshore (~22 m deep) buoys over the 25-hour storm period. A time-series of the integrated wave parameters (Fig. 8) shows the model is able to reproduce the phase of the time-variation, but under predicts the peak H_{m0} values nearshore, while the peak in T_p is under predicted offshore. The overall agreement (*RMSE*) is considered to be good and the maximum values (*Peak Bias*) are acceptably hindcast. The models perform better offshore than nearshore, where improved representation of the physics, and maybe improved spatial resolution, is required. Although the Triaxys wave period data is shown, gaps occur in the data, where inaccuracies due to errors in the firmware (currently under investigation) are suspected. The inclusion of 2D radiation stress (PW-2Dr, Fig. 8) has a small effect on the water levels at these locations, thus the wave predictions are practically the same as if radiation stress had not been considered (PW, Fig. 8) so do not produce much change in the model skill statistics (Table 3).

3.4 Nearshore Interactions

The PW-2Dr simulation is used to determine if any significant interaction and relationships between the wave setup and the tide, wave heights or surge exist. The interaction between the tidal, wave and storm induced increased water levels (meteorological surge and wave setup) is similar to that found by Kim et al. (2008); the maximum meteorological surge and maximum wave setup do not occur at high water, while maximum nearshore wave heights do occur close to high water. In this case the maximum wave setup occurs at low water due to the maximum gradient in radiation stress occurring at this time, discussed below.

The correlation (R^2) is calculated to determine the existence of any linear relationship between the different nearshore parameters. A value close to 1 indicates strong correlation. In these circumstances either an interaction and/or dependency between processes can be inferred. Similar trends and the R^2 values in Figure 9(a and c) clearly show that wave setup is dependent on the difference in wave heights between nearshore and offshore. No tidal interaction with wave setup is observed through the correlation with the tide itself or by considering the nearshore (Triaxys) wave height, which is tidally modulated (Fig. 9a). There is a moderate correlation with the offshore wave field and surge, which both peak simultaneously in response to the wind. The correlation is greater with the offshore wave field than with the nearshore field. This is due to the offshore wave heights having a similar time evolution to the spatial gradient (difference) in wave heights across the nearshore zone (and hence momentum flux). The maximum wave setup occurs just after the maximum surge and wave height, as it is not dependent on the peak in wave conditions alone. This lower tidal level is when gradients in the wave conditions and therefore the net momentum flux (radiation stress), are greatest during the storm period. The gradients in momentum flux are caused by wave shoaling in intermediate water and energy dissipation in shallow water. There is a slight dip in the peak value of the difference between wave heights nearshore and offshore (Fig. 9a) in response to the tidal influence and the decaying offshore wave height.

The tide has a large effect on the nearshore wave heights, therefore influencing the gradients in wave conditions (momentum flux). These gradients are greatest at mid to lower water levels (as seen in the difference in wave height, (Fig 9a) causing a peak in wave setup to occur at this time (Fig. 9c). The wave-induced current field and wave-induced elevation across the domain are shown in Figure 10 at 4 stages of the tide cycle: high water, mid water on the falling tide, low water and mid water on the rising tide. The main changes in response to the tidal phase are due to drying banks within the estuaries and depth changes over shoals along the coastline between the Dee and Ribble. The maximum wave setup increases as the tidal level falls (from ~0.05 m to ~0.9 m), and becomes focused within the estuary channels as well as covering a wider cross-shore area along the coast. This is due to the inshore waves being reduced more at lower total water depths increasing the nearshore gradients in the wave momentum flux. On the rising tide (Fig. 10b) the wave setup in the Dee is less than during the falling tide (Fig. 10d), due to the timing of the storm and tidal influence (Fig. 9, 14 hrs and 20.5 hrs). However in the Ribble it is larger on the rising tide (Fig. 10d), most likely due to the NE propagation of the storm still having an impact further north along this coastal area. The wave setup is largest in the Ribble during high water levels when waves are able to propagate over the banks at the mouth and rapidly shoal within the estuary. This is due to the Ribble being the shallowest of the 3 estuaries. During lower water levels, wave setup is greatest in the Dee, when the waves are confined to the deep Dee estuary channels. The restricted entrance to the Mersey and shallow depths surrounding the entrance to the Ribble act to limit wave activity within these two estuaries. Increased levels of wave setup occur during lower water levels, especially over the shallow ebb-shoal banks close to the estuary mouth of the Mersey and Dee. At high water, wave setup is minimal, with a larger effect within the estuaries than at the coast. At the coast, wave attenuation is reduced during higher water levels, thus reducing gradients in the nearshore wave field and therefore wave setup. Continued wave shoaling within the Ribble and Dee estuaries causes larger gradients in the wave field and therefore wave setup, which is able to persist up to the estuary head. In the Dee the wave setup continues to increase within the estuary. In the Mersey it remains constant within the estuary, having a low value due to limited wave activity as a result of the much longer narrower estuary shape with more restricted mouth. In the Ribble, wave setup increases with distance into the estuary and only in the upper reaches does the wave setup start to decrease, where the estuary morphology is dominated by the shallow narrow river channels. At low water the large wave setup at the estuaries mouth rapidly decays towards the estuary head. Wave shoaling in intermediate depths also causes a small (< 2 cm) set-down seaward of wave breaking and the onset of wave setup (Longuet-Higgins and Stewart, 1964). At mid and low water levels set-down becomes evident in the nearshore region moving between approximately the 20 m and 10 m depth contours depending on the state of the tide.

The maximum values of the depth-averaged wave-induced current field across the model domain occur alongshore and in areas of shallow banks (Fig. 10). Simulated wave-induced current speeds are of the order of 0.2 m/s reaching maximum values of 0.5 m/s for this event. The wave-induced currents are greatest during the falling tide and low water. Again this period is when radiation stress has greatest influence, as demonstrated in Figure 9c for wave setup. The areas of largest wave-induced currents are in the regions of the nearshore shoals and close to the coast, demonstrating the important influence of the bathymetry on the gradients of the radiation stress. These patterns in current magnitude become larger with the falling tide, as shoals have greater influence on the wave field and also steer the flow. The wave-induced currents are generally directed onshore-offshore (east-west) in the open nearshore region surrounding Site A. On the falling tide there is a clear offshore flow in the main entrance channel of the Mersey (Fig. 10f). It is likely this flow is a return flow in response to the wave setup over the shallow banks. The currents generated alongshore are generally southerly past the Ribble and converge in the Dee and Mersey. A divergence is also found at the tip of the Great Orme (located in Fig.1).

4. Discussion

This research sets out to investigate the importance of radiation stress during an extreme storm event in a shallow wave-influenced region and to properly assess the validity of the 2D method, while the more complex 3D implementations are still subject to debate and computationally more expensive. This is achieved by extending an existing coupled wave and circulation model to include radiation stress in 2D. By comparison with observations, the procedure is found to be both robust and efficient. It is demonstrated that including 2D radiation stress in POLCOMS-WAM gives a good hindcast of wave, current, surge and wave setup variables across the complex shallow water region of open coast and enclosed estuaries. This 2D method also remains stable across this complex coastal domain, whereas the applicability of 3D methods to the full domain is questionable, and give much larger values of wave setup (see Brown, 2010). Wave setup (and related alongshore drift) is found to have most impact along the coastline and over shallow banks at the mouths of the estuaries, making it an important process to consider in storm forecasting (or hindcasting) in regions of wave influence. Over shallow and intertidal areas wave setup may modify the inundation, influencing the tide-surge-wave impact on these regions. Comparison of the maximum wave height (Fig. 4a) with those found by Brown (2010), show the wave field in shallow (estuarine and coastal) regions can attain slightly larger maximum values due to wave setup increasing the total water depth. Any increase in the total water level potentially alters the position of wave action relative to the shore/estuary profile. Over shallow (bank) regions the residual circulation and inundation of low-lying areas could be modified as well as the wave field, changing the sediment transport due to wave-circulation interaction and the risk due to erosion and flooding during the storm impact.

To correctly disperse the radiation stress within enclosed (estuary) regions 2-way coupling between circulation and wave models is required to prevent artificially sustained setup. It is found that the largest wave setup is focused over shallow banks in the estuaries mouth and along the Sefton and North Wirral coasts (Fig. 4b). In the upper estuaries wave activity is smaller and the setup diminishes. Along the open coast wave setup is restricted to the very nearshore zone; while offshore the water level is relatively unchanged. Although wave setup has a relatively small contribution at the tide gauge locations (~ 0.07 m contribution, Fig. 4b), which are sheltered from wave activity and generally rather deep, and along the coast (~ 0.09 m contribution, Fig. 4b), it can be considered important over shallow banks at an estuary mouth in wave-dominant areas, for example (Fig. 4b) it reached values up to 0.15 m at the Ribble mouth (approximately 8% of the observed 2 m surge level at Liverpool). It is demonstrated that wave setup is important at the coast and may need to be considered in operational modelling, for accurate surge forecasts along the open coast in regions of significant wave activity. However, the maximum wave setup in this case occurs at low water levels and the maximum total water level is relatively unchanged. For improved validation, observations in shallow water at the open coast are required, where both the meteorologically- and wave-induced surge components are important, since tide gauges are often situated in deep and sheltered locations. With distance from the coast towards the offshore the surge reduces in magnitude, although less rapidly than the wave setup. Surge models are often developed using tide gauge data for validation, since long-term data sets are readily available and accurate forecasting at the coast is most important for warning systems. For this event POLCOMS has greater accuracy at the coast than offshore (Table 1). Long-term offshore observation is therefore required, to validate (and tune) existing surge models to capture the regional offshore extent of the surge and not just the coastal influence. Some of the over-prediction seen in the offshore surge hindcast (Fig. 3) could be the result of the method being used to remove the tide, but may also be due to low resolution meteorological forcing not capturing the variability in offshore and nearshore (wind) conditions during a storm (Bricheno et al., 2013).

POLCOMS-WAM without radiation stress is shown to accurately simulate the nearshore current field (Table 2), and is only slightly modified by the inclusion of radiation stress. At Sites A and B (depths ≈ 25 m) wave-induced currents are weak. However the currents are larger at the shallower site (A) implying that closer to the shore consideration of these currents becomes more important. This again demonstrates the need for more nearshore coastal data, where radiation stress is important, inducing currents and setup. Analysis of the modelled wave-induced current profiles (Fig. 6) shows that wave-induced currents are most influential in the upper half of the water column and become more significant during the lower water levels from mid to low tide, when the gradients in the wave field (wave momentum flux) are greatest. The vertical current profile formed when using 2D radiation stress in a 3D circulation model implies that the more computationally expensive 3D methods may not be significantly advantageous for modelling storm conditions (operationally) in intermediate water depths. However, in some regions, or under certain condition, the wave-induced current could have an important influence on the vertical current profile and so there is still need for 3D methods, which are appropriate for use in regional models. The wave-induced currents during this storm event are found to be important along the coast and at the mouths of estuaries (Fig. 10). During high water levels the wave-induced currents are mainly alongshore, while at low water levels a complex onshore-offshore circulation occurs in shallow regions of the nearshore. This is most likely to be in response to increased water levels within the estuary domains. The long-term wave-induced current pattern due to the storm climate is likely to be of importance when considering the coastal sediment transport and morphological storm impact for this location, as found at other shallow locations (e.g. Brown and Davies, 2009). It is inferred that in Liverpool Bay these currents are likely to redistribute and exchange sediment between the banks at estuary mouths during storm conditions, if not during milder wave conditions as well. The direction of the wave-induced currents (Fig. 10e – g) implies that any sediment drift during southwest to westerly storms will be towards the mouth of the Dee and Mersey. Holden et al. (2010) show the long-term sediment transport to diverge at Formby Point towards north and south, as does the flood tidal current, which has a dominant east-west component. This implies that storms enhance the net tidal transport pattern south of Formby Point and inhibit it north of Formby Point. During storm events the wind induced currents also become important in shelf seas (e.g. Wang et al., 2012), potentially being more important than wave-driven circulation further offshore.

Wave height, wave setup, tidal elevation and surge elevation have been used to investigate the tide-surge-wave interactions. Wave setup is shown to depend strongly on the gradients in the wave field, which are caused by wave shoaling and dissipation. Although wave setup can increase the surge levels, due to tidal modulation of the nearshore wave conditions, the largest possible gradients in wave momentum flux occur close to low water, creating the maximum wave setup when the threat of flooding is low. The significance of the contribution of wave setup to increasing flood risk may therefore be related to the tidal range of a region. The tide also plays an important role in the location of the surf zone over intertidal areas. Brown (2010, Fig. 9) shows the variable position of the wave field at different stages of the tide. Here it is shown that the changing tidal elevations greatly influence the position, area of influence and magnitude of wave setup and wave-induced current patterns across Liverpool Bay (Fig. 10). At low water, the area and magnitude of setup is greatest, but the impact may be least important. Consideration of wave-induced currents is thought to be important in determining sediment pathways during a storm event. Although these currents are approximately 10-30% of the tidal current speed at the coast, they will contribute to the weaker time-averaged current residual during the storm period.

Comparison of the computation times shows that inclusion of the 2D radiation stress has no impact on the simulation time of POLCOMS-WAM; while 3D methods (applied by Brown et al., 2011) increase it (by approximately 25%). The 2D method can be included within the standard version of WAM that only considers 2D depth-averaged currents rather than depth-integrated currents over a depth of wave influence (see Brown et al., 2011), which is considerably more efficient (saving about 1 hour per simulated day). The results presented show that accurate tide-surge-wave conditions can be simulated without consideration of the vertical structure of the radiation stress profile. This is not surprising as surface elevation is related to the depth integrated currents, but for sediment transport modelling an accurate vertical current profile is more likely to be required.

One further point of discussion is the method used to obtain the surge (tidal residual) at the offshore sites. Liverpool Bay is an area where shallow water is considered to have significant influence on the tidal dynamics making short-term data difficult to analyse (Brown et al., 2012). Both shallow water and major tidal constituents are therefore used, in an accurate tidal analysis, to remove the tidal signal from the total observed elevation to obtain the surge residual. Any tidal analysis package assumes the mean residual to be (approximately) zero over the analysis period, which can be invalid. The mean can vary, due to seasonal, inter- and intra- annual effects. Over very long periods the mean can be assumed to be zero. At coastal tide gauge sites, observations have been collected for many years, so this assumption is valid, thus giving accurate tidal residuals. However at offshore sites, continuous observation is often over short periods (one to a few months), so although a good approximation of the tides and surge is obtained the mean (absolute) water level will be non-zero. Due to the short simulation period in this study, the 25-hour mean storm residual is used to correct the data. The shift is 0.43 m in the case of PW and PW – 2Dr at Site A, and 0.40 m at Site B. To enable more reliable surge observations offshore, either a longer model simulation is needed to correct the observed mean over, say, a monthly period, or longer continuous periods of observation are required at offshore locations. Here, the offshore observation implies that the model over-predicts the surge offshore, but this cannot be considered as absolute since inaccuracy in the adjustment of the mean is likely. However the observations show that the model simulates the reduction in the surge and the tidal modulation with distance from the coast.

5. Conclusion

A tide-surge-wave model (POLCOMS-WAM) of Liverpool Bay, UK, has been modified to include radiation stress using the 2D method of Mastenbroek et al. (1993). The results have been used to consider the impact of radiation stress across this region. The 2D method gives accurate wave-induced depth-average current and water levels, and has been shown to generate a realistic depth-varying influence nearshore when implemented in a 3D circulation model. However, 3D methods are still needed to accurately represent the 3D current structure, especially in regions of complex depth-variation in the current field (e.g., within the lower estuary region). Through validation with observations where possible over the domain, it is found that a 2D method suffices for efficient and acceptable hindcast of storm conditions using POLCOMS-WAM. The 2D methodology is not only accurate and robust within a complex region, but has also proven to be a computationally efficient method. If implemented in a 3D hydrodynamic model some variations in the vertical profile of the wave-induced currents will still occur. Here (Fig. 6) the wave-induced currents are larger towards the surface in response to the depth-averaged forcing.

The hindcast extreme storm event demonstrates that in shallow nearshore regions affected by waves, wave setup is influential at low water elevations and wave-induced currents are important. Water levels are typically increased by < 0.09 m (Fig. 4b) by wave setup, while the meteorological surge (< 2 m) is the dominant process in this location (Fig. 4c). An additional wave-driven coastal current is generated with typical speeds of 0.15 m/s (Fig. 10 e-f), which is ~

15% of the observed total current (< 1 m/s, Fig. 5) in this case. Further offshore and in the upper estuary region these processes are not so important. The model comparison also demonstrates that the influence of wave setup is not captured at tide gauge location due to their deep and sheltered nature. The results of this study demonstrate that along the shallow areas of open coast radiation stress is an important process to consider as it contributes to the time-averaged residual current patterns, especially at low water levels. For this coastal domain, the maximum (< 8%) wave-surge setup contribution to the surge levels at the open coast tend not to occur at tidal high water. It is therefore suggested that in macrotidal conditions, wave setup may not drastically increase flood risk, which is greatest at tidal high water.

Acknowledgments

This research was initiated as part of the MICORE (EU FP7 program grant 202798), FORMOST (NERC grant NE/E015026/1) and FIELD_AC (EU FP7 program grant 242284) projects and has been completed as part of the iCOASST (NERC grant NE/J005444/1) and ARCoES (EPSRC, ARCC-CN programme grant EP/I035390/1) projects. The support of the European Commission through FP7, contract 288710 – MERMAID, is gratefully acknowledged. NOC colleague Jane Williams and the UK Met Office are thanked for providing meteorological model data to force the models for this study period. Jane also supplied operational surge model output to account for the external surge. The PROMISE partners are acknowledged for initial code development, coupling M93 in 1-way within WAM. Without the valuable observations from BODC, COBS and CEFAS model validation would not have been possible.

References

Ardhuin, F., Jenkins, A.D., Belibassakis, K.A., 2008a. Comments on “The three-dimensional current and surface wave equations”. Journal or Physical Oceanography, 33(9), 1340−1350.

Ardhuin, F., Rascle, N., Belibassakis, K.A., 2008b. Explicit wave-averaged primitive equations using a generalized lagrangian mean. Ocean Modelling, 20(1), 35–60.

Ashworth, M., Holt, J.T., Proctor, R., 2004. Optimization of the POLCOMS hydrodynamic code for terascale high-performance computers. Proceedings of the 18th International parallel and distributed processing symposium, 26th–30th April, Santa Fe, New Mexico.

Bennis, A-C., Ardhuin, F., Dumas, F., 2011. On the coupling of wave and three-dimensional circulation models: Choice of theoretical framework, practical implementation and adiabatic tests, Ocean Modelling, 40(3–4), 260–272.

Bennis, A-C., Ardhuin, F., 2011. Comments on “The Depth-Dependent Current and Wave Interaction Equations: A revision”. Journal or Physical Oceanography, 41(10), 2008–2012.

Bolaños, R., Wolf, J., Brown, J., Osuna, P., Monbaliu, J. and Sánchez-Arcilla, A. 2009. Comparison of wave-current interaction formulation using POLCOMS-WAM wave-current model. Coastal Engineering, 521–533 pp. World Scientific Publishing, ISBN: 13 978-981-4277-36-5

Bolaños, R., Brown, J.M., Souza, A.J. 2011a. Three dimensional circulation modeling in the Dee Estuary. Journal of Coastal Research, SI(64), 1457-1461.

Bolaños, R., Osuna, P. Wolf, J., Monbaliu, J. and Sanchez-Arcilla, A., 2011b. Development of POLCOMS-WAM model. Ocean Modelling. 36(1–2), 102–115.

Booij, N., Ris, R.C., Holthuijsen, L.H., 1999. A third-generation wave model for coastal regions, Part I, Model description and validation. Journal of Geophysical Research, 104 (C4), 7649–7666.

Bricheno, L.M., Soret, A., Wolf. J., Jorba, O., and Baldasano, J.M., 2013. Effect of high-resolution meteorological forcing on nearshore wave and current model performance. Journal of Atmospheric and Oceanic Technology, in press.

Brown, J.M., 2010. A comparison of WAM and SWAN under storm conditions in a shallow water application. Ocean Modelling, 35(3), 215–229.

Brown, J.M., Bolaños, R., Howarth, M.J., Souza, A.J., 2012. Extracting sea level residual in tidally dominated estuarine environments. Ocean Dynamics, 62(7), 969–982.

Brown, J.M., Bolaños, R., Wolf, J., 2011. Impact assessment of advanced coupling features in a tide-surge-wave model, POLCOMS-WAM, in a shallow water application. Journal of Marine Systems, 87(1), 13–24.

Brown J.M., Davies, A.G. 2009. Methods for medium-term prediction of the net sediment transport by waves and currents in complex coastal regions. Continental Shelf Research, 29(11–12), 1502–1514.

Brown, J.M., Souza, A.J., Wolf J., 2010. An 11-year validation of wave-surge modelling in the Irish Sea, using a nested POLCOMS-WAM modelling system. Ocean Modelling, 33(1–2), 118–128.

Brown J.M., Wolf J., 2009. Coupled wave and surge modelling for the eastern Irish Sea and implications for model wind-stress. Continental Shelf Research, 29(10), 1329–1342.

Dean, R.G., Bender, C.J., 2006. Static wave setup with emphasis on damping effects by vegetation and bottom friction, Coastal Engineering, 53(2–3), 149–156.

Dietrich, J.C., Tanaka, S., Westerink, J.J., Dawson, C.N., Luettich Jr, R.A., Zijlema, M., Holthuijsen, L.H., Smith, J.M., Westerink, L.G., Westerink, H.J., 2012. Performance of the unstructured-mesh, SWAN+ADCIRC model in computing hurricane waves and surge, Journal of Scientific Computing, 52(2), 468–497.

Flather, R.A., 1994. A storm surge model of the northern Bay of Bengal with application to the cyclone disaster in April 1991. Journal or Physical Oceanography, 41(1), 172−190.

Harris, D.L., 1963. Characteristics of hurricane storm surge. Washington, D.C, U.S. Department of Commerce, Weather Bureau. Technical Paper No 48/ 139pp.

Holden, V., Worsley, A., Lymbery, G., Pugh, C., 2010. The Sefton coast conceptual model, north coast summary report, Edge Hill University, 8pp.

Holt, J.T., James I.D., 2001. An s coordinate density evolving model of the northwest European continental shelf: 1, Model description and density structure. Journal of Geophysical Research, 106(C7), 14,015−14,034.

Howarth, M.J., Proctor, R., Knight, P.J., Smithson, M.J., Mills, D.K., 2006. The Liverpool Bay Coastal Observatory :towards the goals. Proceedings of Oceans ’06, MTS/IEEE, Boston: 6pp., doi: 10.1109/OCEANS.2006.307095

Kim, S.Y., Yasuda, T., Mase, H., 2008. Numerical analysis of effects of tidal variations on storm surges and waves. Applied Ocean Research, 30(4), 311–322.

King, B.A., Blackley, M.W.L., Carr, A.P., Hardcastle, P.J., 1990. Observations of wave-induced set-up on a natural beach. Journal of Geophysical Research, 95(C12), 22289-22297.

Komen, G.J., Cavaleri, L., Donelan, M., Hasselmann, K., Hasselmann, S., Janssen, P.A.E.M., 1994. Dynamics and modelling of ocean waves. Cambridge University Press, Cambridge, 532pp.

Kumar, N., Voulgaris, G., Warner, J.C., 2011. Implementation and modification of a three-dimensional radiation stress formulation for surf zone and rip-current applications. Coastal Engineering, 58(12), 1097–1117.

Kumar, N., Voulgaris, G., Warner, J.C., Olabarrieta, M., 2012. Implementation of the vortex force formulism in the coupled ocean-atmosphere-wave-sediment transport (COAWST) modelling system for inner shelf and surf zone applications. Ocean Modelling, 47, 65–95.

Longuet-Higgins, M.S., 1970a. Longshore currents Generated by Obliquely Incident Sea Waves, 1. Journal of Geophysical Research, 75(33), 6778–6789.

Longuet-Higgins, M.S., 1970b. Longshore currents Generated by Obliquely Incident Sea Waves, 2. Journal of Geophysical Research, 75(33), 6790–6801.

Longuet-Higgins, M.S., Stewart, R.W., 1964. Radiation stresses in water waves; a physical discussion with applications. Deep-Sea Research, 11, 529–562.

Mastenbroek, C., Burgers, G., Janssen, P.A.E.M., 1993. The dynamical coupling of a wave model and a storm surge model through the atmospheric boundary layer. Journal of Physical Oceanography, 23(8), 1856−1866.

Mellor, G., 2003. The three-dimensional current and surface wave equations. Journal of Physical Oceanography, 33(9), 1978–1989.

Mellor, G., 2005. Some consequences of the three-dimensional current and surface wave equations. Journal of Physical Oceanography, 35(11), 2291–2298.

Mellor, G., 2008. The depth-dependent current and wave interaction equations: a revision. Journal of Physical Oceanography, 38(11), 2587–2596.

Mellor, G., 2011a. Wave radiation stress. Ocean Dynamics, 61(5), 563–568.

Mellor, G., 2011b. CORRIGENDUM. Journal of Physical Oceanography, 41(7), 1417–1418.

Mellor, G., 2011c. Reply to comments by A-C Bennis and F. Ardhuin. Journal of Physical Oceanography, 41(10), 2013–2015.

Mellor, G., 2013. Waves, circulation and vertical dependence. Ocean Dynamics, 63(4), 447–457.

Moghimi, S., Klingbeil, K., Gräwe, U., Burchard, H., (in press). A direct comparison of a depth-dependent Radiation Stress formulation and a Vortex force formulation within a three-dimensional coastal ocean model. Ocean Modelling, available online 7^{th} November 2012.

Monbaliu, J., Padilla-Hernández, R., Hargreaves, J.C., Carretero-Albiach, J.C., Luo, W., Sclavo, M., Günther, H., 2000. The spectral wave model WAM adapted for applications with high spatial resolution. Coastal Engineering, 41(1−3), 41−62.

Osuna, P., Wolf, J., 2005. A numerical study of the effect of wave-current interaction processes in the hydrodynamics of the Irish Sea, International Conference on ocean Waves and Analysis. WAVES, Madrid, Spain.

Ozer, J., Padilla-Henandez, R., Monbaliu, J., Alvarez Fanjul, E., Carretero Albiach, J.C., Osuna, P., Yu, J.C.S., Wolf, J., 2000. A coupling module for tides, surge and waves. Coastal Engineering 41(1–3), 95–124.

Pawlowicz, R., Beardsley, B., Lentz, S. 2002. Classical tidal harmonic analysis including error estimates in MATLAB using T_TIDE. Computers and Geosciences, 28(8), 929–937.

Pleskachevsky, A., Eppel, D.P. and Kapitza, H. 2009. Interaction of waves, currents and tides, and wave-energy impact on the beach area of Sylt island. Ocean Dynamics, 59(3), 451–461.

Roland, A., Cucco, A., Ferrarin, C., Hsu T., Liau, J., Ou, S., Umgiesser, G. and Zanke, U. 2009. On the development and verification of a 2-D coupled wave-current model on unstructured meshes. Journal of Marine Systems, Volume 78, Supplement 1, November 2009, Pages S244-S254

Sheng, Y.P., Zhang, Y. and Paramygin, V.A. 2010. Simulation of storm surge, wave, and coastal inundation in the Northeastern Gulf of Mexico region during Hurricane Ivan in 2004. Ocean Modelling, 35(4), 314–331.

Sheng, Y.P., Liu, T., 2011. Three-Dimensional Simulation of Wave Induced Circulation – Comparison of Three Radiation Stress Formulations. Journal of Geophysical research, 116(CO5021), 17pp.

Sherman, D.J. 1988. Empirical Evaluation of Longshore-Current Models. The Geographical Review, 78(2), 158–168.

Tucker, M.J., Pitt, E.G. 2001. Waves in Ocean Engineering. Elsevier Ocean Engineering Book Series, vol. 5, Amsterdam, Elsevier. 548p.

Xia, H., Xia, Z. and Zhu, L. 2004. Vertical variation in radiation stress and wave-induced current. Coastal Engineering, 51(4), 309–321.

Xie, L., Liu, H. and Peng, M. 2008. The effect of wave-current interactions on the storm surge and inundation in Charleston Harbour during Hurricane Hugo 1989. Ocean Modelling, 20(3), 252–269.

Wang, Z.B., Hoekstra, P., Burchard, H. Ridderinkhof, H. ., De Swart, H.E., Stive, M.J.F. 2012. Morphodynamics of the Wadden Sea and its barrier island system. Ocean & Coastal Management, 68(Special Issue on the Wadden Sea Region), 39–57.

Figure captions:

Fig. 1. a) The ~180 m Liverpool Bay model domain, nested with the ~1.8 km Irish Sea model, in turn nested within the ~12 km Continental Shelf model. b) Bathymetry contours are relative to mean tidal level (MTL) and the symbols represent observation stations. Tide gauges are marked with triangles, wave buoys are marked by circles and the fixed moorings with ADCP are marked with stars.

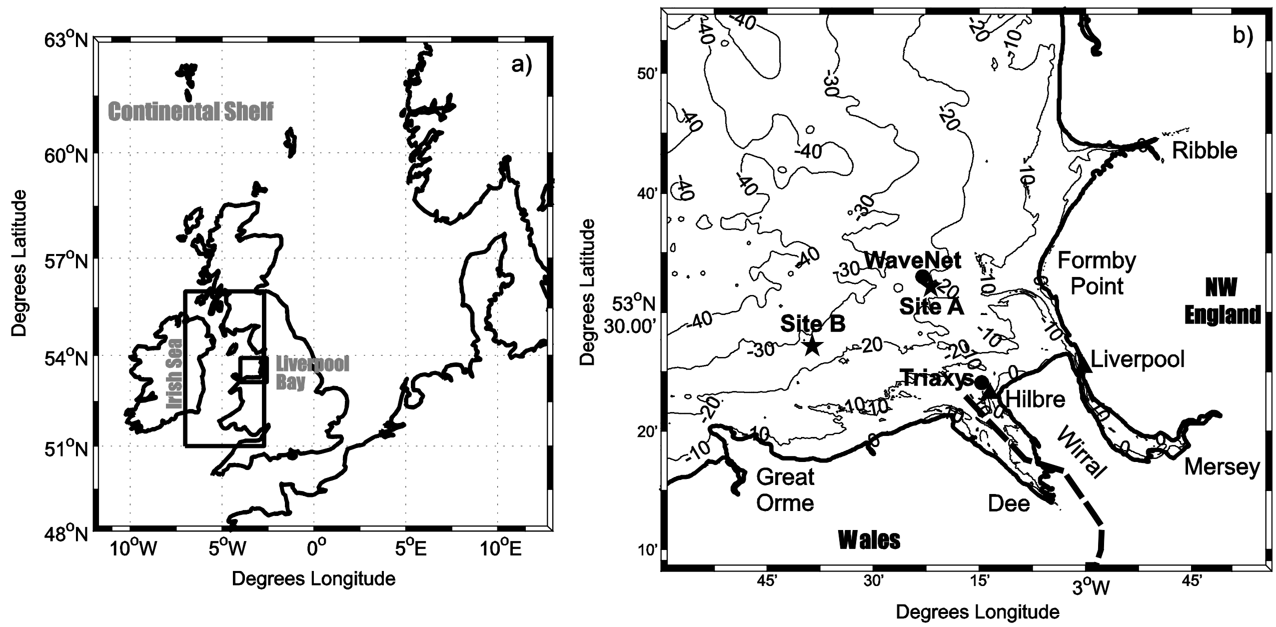

Fig. 2. The observed and hindcast surge at Hilbre (a) and Liverpool (b). All model setups, identified in Table 1, are shown. The time series over the 25 hour storm period starts 00:00 18th January and ends 00:00 19th January.

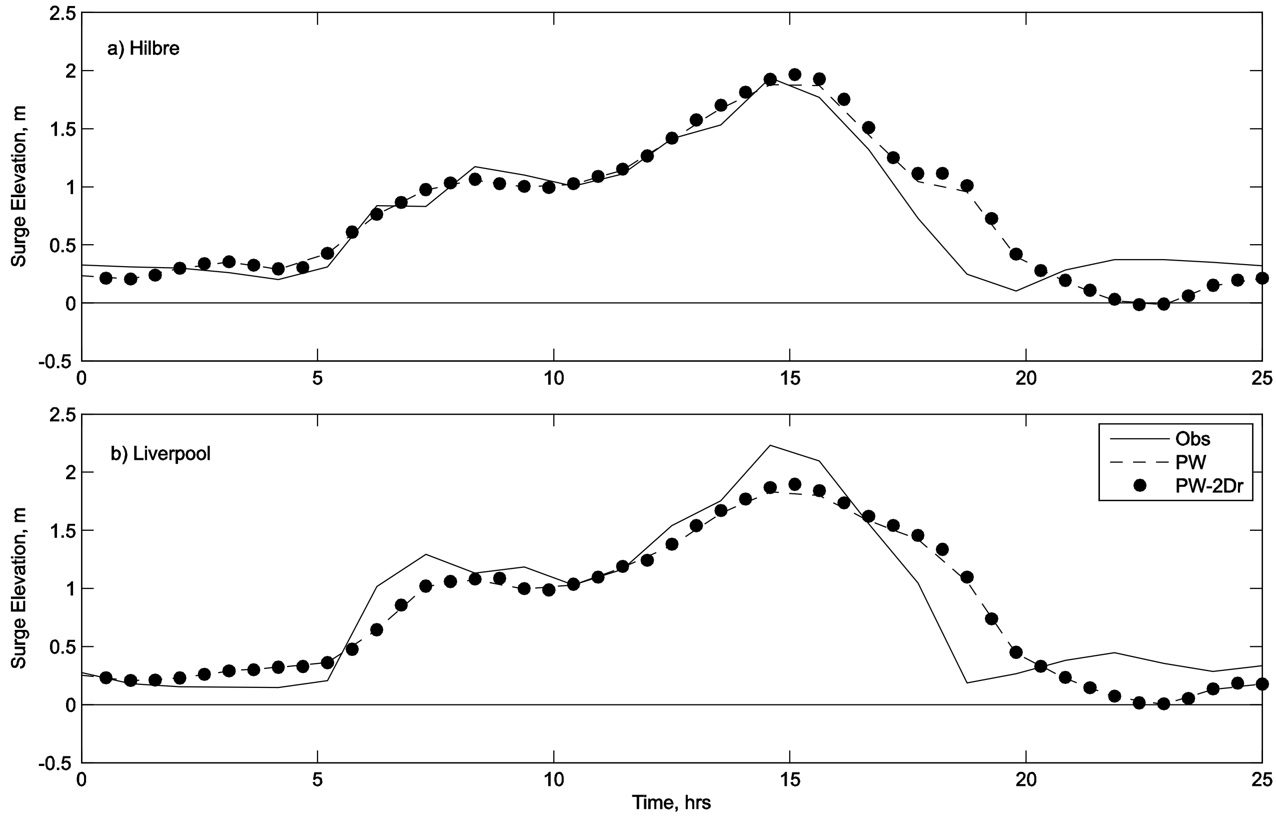

Fig. 3. The observed (corrected to the PW mean value) and hindcast surge at Site A (a) and Site B (b). All model setups, identified in Table 1, are shown. The time series over the 25 hour storm period starts 00:00 18th January and ends 00:00 19th January.

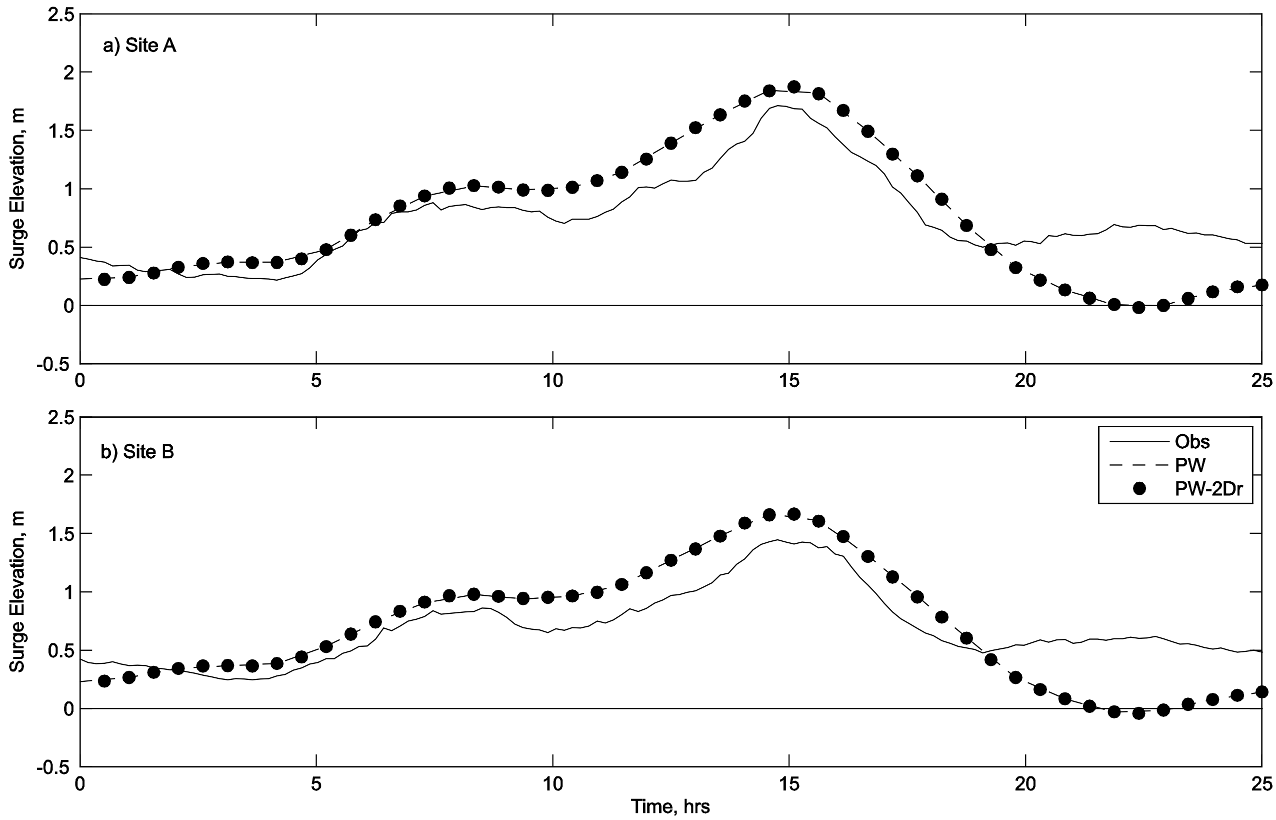

Fig. 4. The maximum significant wave height, m (a), maximum wave setup, m (b) and the ratio of the maximum wave setup to the maximum meteorological surge (c), all at each grid point across the model domain, occurring at independent times during the 25 hour storm period.

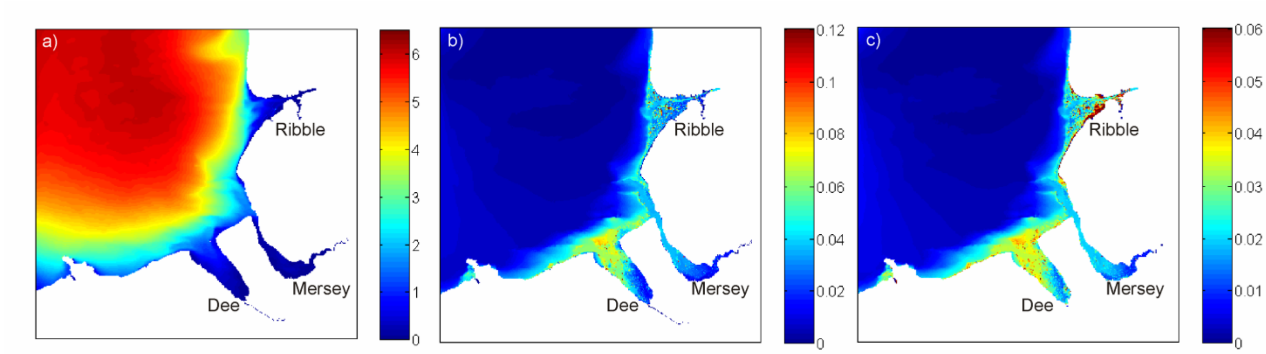

Fig. 5. Profiles of the observed and POLCOMS-WAM modelled time-varying horizontal velocity (m/s) over the 25 hour storm period at the two instrumented mooring Sites A and B, starting 00:00 18th January ending 00:00 19th January. The model simulations are with and without the inclusion of 2D radiation stress. The velocity components to the east and north are represented by *u* and *v* respectively. In the top panels the surface elevation is shown.

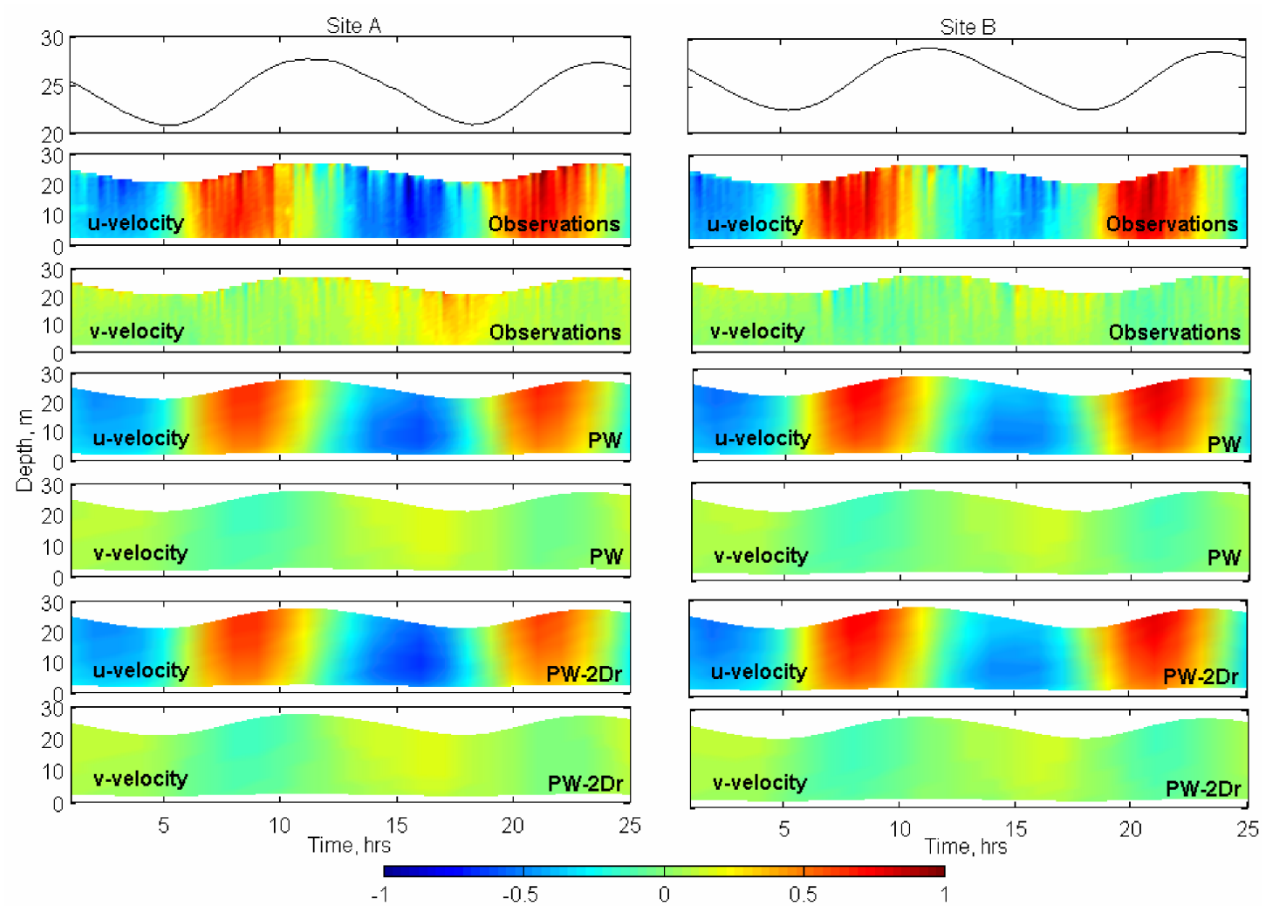

Fig. 6. The POLCOMS-WAM modelled vertical profile of the wave-induced velocity components over the 25 hour storm period at the two instrumented mooring Sites A and B, starting 00:00 18th January ending 00:00 19th January. The model simulation includes 2D radiation stress methods as identified in Table 1 and validated in Table 2. The velocity components to the east and north are represented by *u* and *v* respectively.

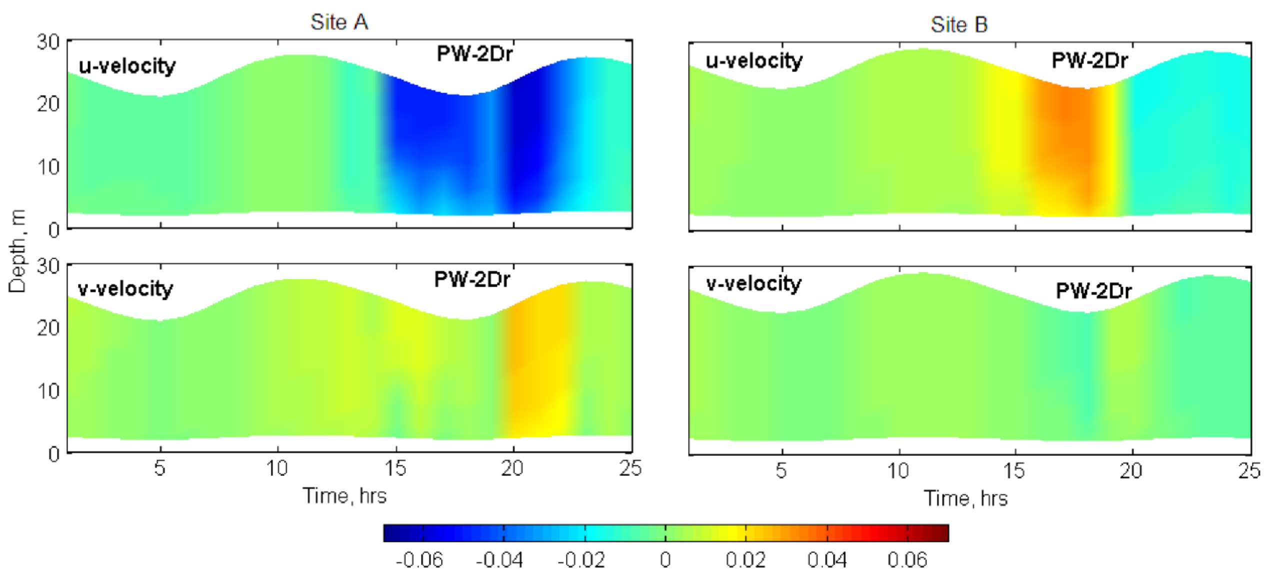

Fig. 7. The POLCOMS-WAM modelled depth-averaged velocities (m/s) over the 25 hour storm period at the two instrumented mooring Sites A and B, starting 00:00 18th January ending 00:00 19th January. The 2D radiation stress method, as identified in Table 1, was used in this model simulation. The velocity components to the east and north are represented by *u* and *v* respectively.

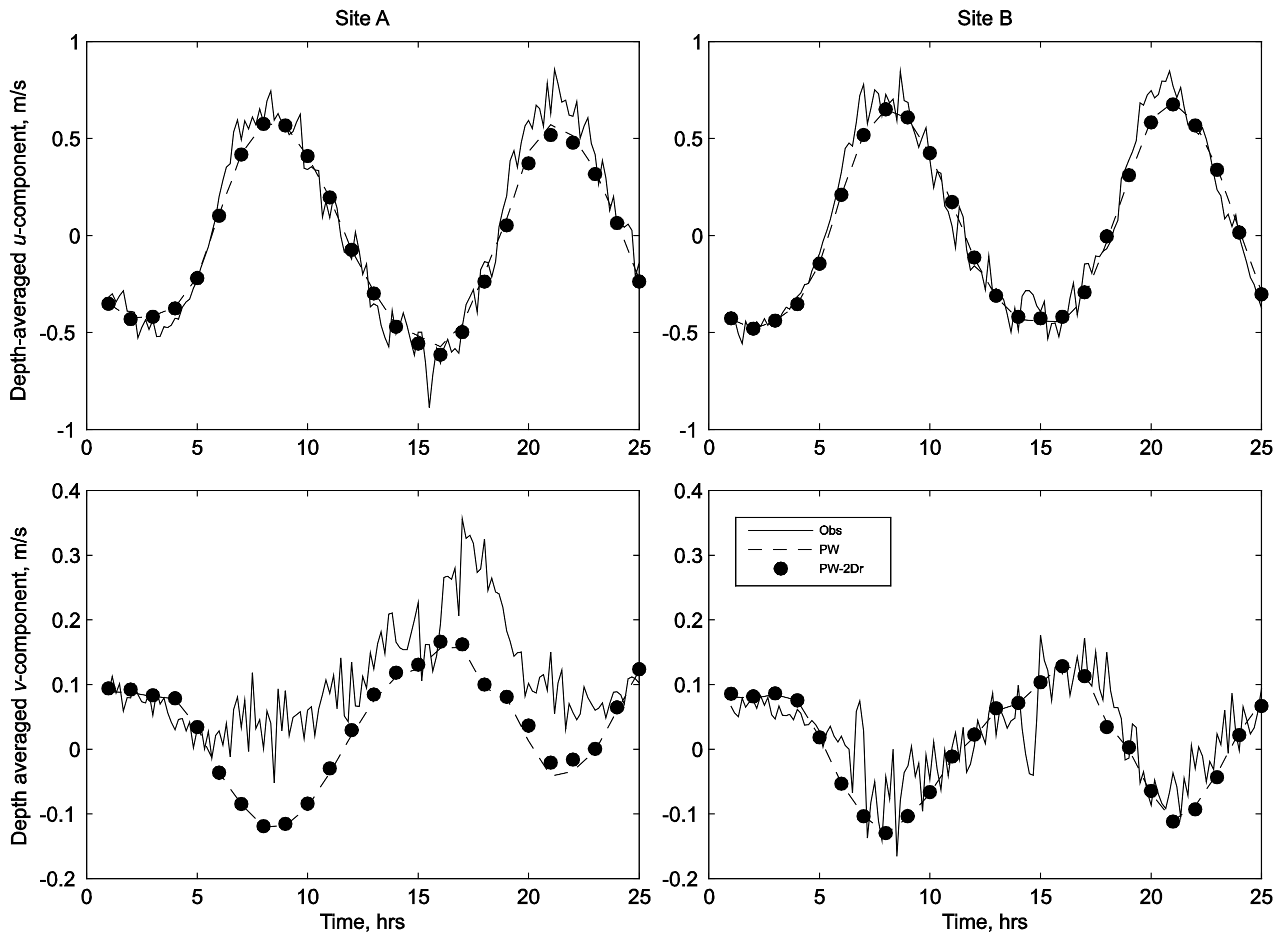

Fig. 8. The observed (obs) and hindcast (PW, PW-2Dr) wave conditions at the WaveNet (left) and Triaxys (right) buoys over the 25 hour storm period, starting 00:00 18th January ending 00:00 19th January. The model setups PW and PW-2Dr can be identified in Table 3.

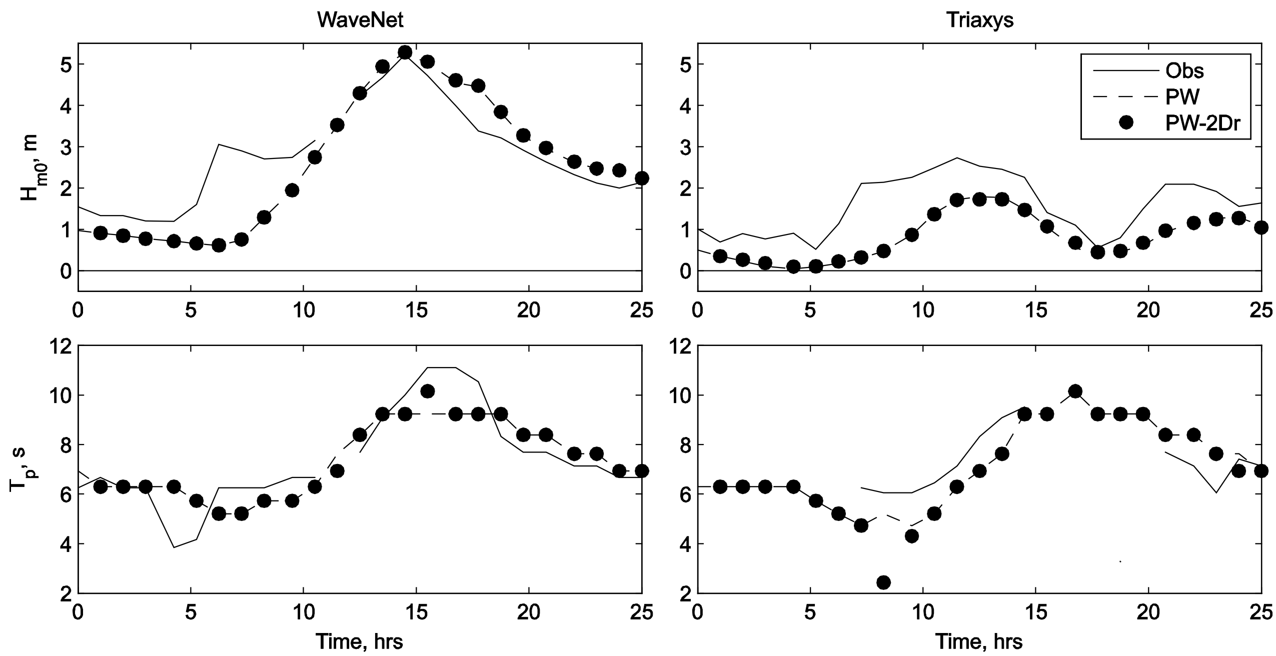

Fig. 9: Time series of modelled nearshore parameters from PW-2Dr at the Triaxys, WaveNet and Hilbre locations, as specified in the legends. The correlation (R^2 value) between each parameter given in the legend in panel a and b is with the wave setup in panel c.

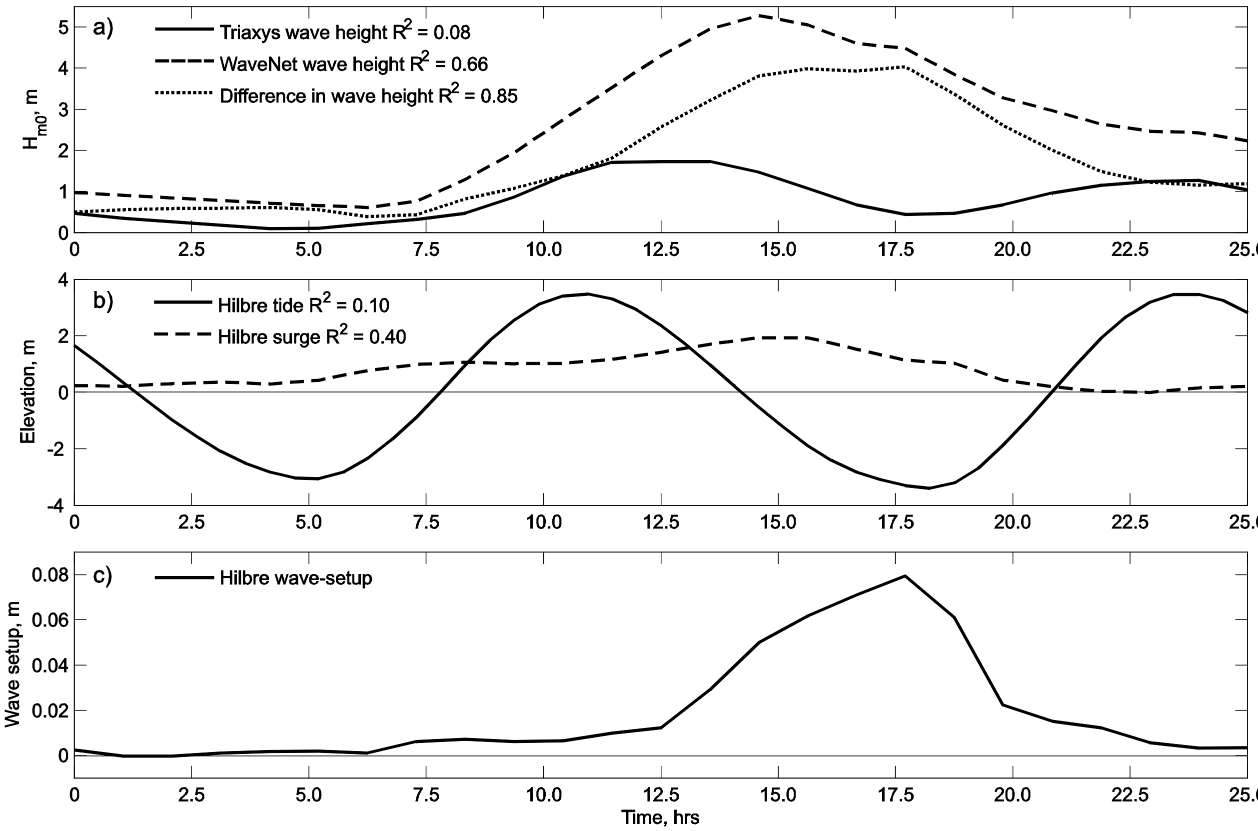

Fig. 10. The wave setup (top row) and depth-averaged wave-induced current speed (bottom row) across the model domain at different stages of the tide during the 25 hour storm period for the PW-2Dr simulation, identified in Table 1.

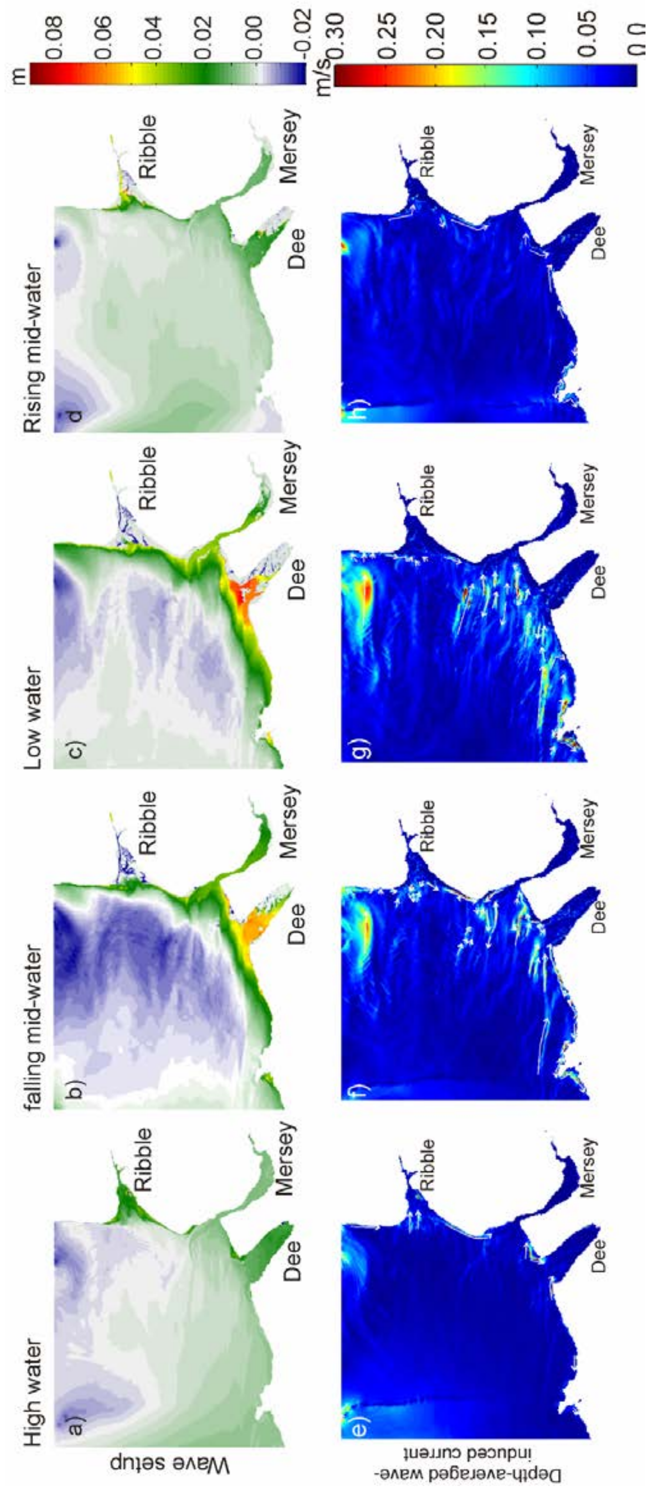

Table Captions:

Table 1: Valiation metrics for surge with and without wave setup, between the model hindcast and observation for: POLCOMS-WAM (PW) and POLCOMS-WAM including 2D radiation stress (PW-2Dr). The observations used to estimate the metrics consist of the total (meteorological and wave-induced) surge. The observation locations are given in Fig. 1. At Site A and B the observations are corrected by the modelled mean residual for each simulated case.

	Hilbre, *surge*		Liverpool, *surge*		Site A, *surge*		Site B, *surge*		Model Run Time (h)
Model coupling	*RMSE* (m)	*Peak Bias* (m)	*RMSE* (m)	*Peak Bias* (m)	*RMSE* (m)	*Peak Bias* (m)	*RMSE* (m)	*Peak Bias* (m)	
PW	0.22	-0.06	0.28	-0.40	0.31	0.15	0.30	0.23	11.6
PW – 2Dr	0.23	-0.01	0.28	-0.36	0.31	0.15	0.30	0.23	11.6

Table 2: Validation metrics for the depth-averaged currents between the model hindcast and ADCP observation for: POLCOMS-WAM (PW) and POLCOMS-WAM including 2D radiation stress (PW-2Dr). The velocity components to the east and north are represented by *u* and *v* respectively. The observation locations are given in Fig. 1.

	Site A, *u*-velocity		Site A, *v*-velocity		Site B, *u*-velocity		Site B, *v*-velocity	
Model coupling	*RMSE* (m/s)	*Mean Bias* (m/s)	*RMSE* (m/s)	*Mean Bias* (m/s)	*RMSE* (m/s)	*Mean Bias* (m/s)	*RMSE* (m/s)	*Mean Bias* (m/s)
PW	0.070	-0.015	0.110	-0.080	0.093	-0.027	0.055	-0.028
PW-2Dr	0.085	-0.02	0.105	-0.074	0.091	-0.024	0.056	-0.028

Table 3: Validation metrics for the significant wave height (H_{m0}), peak period (T_p) mean period (modelled T_{m02}, observed T_z) between the model hindcast and observation for: POLCOMS-WAM (PW) and POLCOMS-WAM including 2D radiation stress (PW-2Dr). The observation locations are given in Fig. 1.

	WaveNet, H_{m0}		Triaxys, H_{m0}		WaveNet, T_p		Triaxys, T_p	
Model coupling	*Peak Bias* (m)	*RMSE* (m)	*Peak Bias* (m)	*RMSE* (m)	*Peak Bias* (s)	*RMSE* (s)	*Peak Bias* (s)	*RMSE* (s)
PW	0.06	0.85	-1.01	0.87	-1.88	0.99	0.63	2.16
PW-2Dr	0.06	0.85	-1.00	0.87	-0.96	0.94	0.63	2.16